International Journal of
INTELLIGENT SYSTEMS AND APPLICATIONS IN ENGINEERING
ISSN:2147-6799 www.ijisae.org Original Research Paper

A Data Driven Deep Neural Network Model for Identifying both Covid-19 Disease along with Potential Pandemic Hotspots

Mr. Sandeep Kumar Mathariya*[1], Dr. Hemang Shrivastava [2]

Submitted: 07/01/2024 **Revised**: 13/02/2024 **Accepted**: 21/02/2024

Abstract: The COVID-19 pandemic was once in a century event with massive losses of human life, along with unprecedented financial and social losses worldwide. Detecting the disease early and accurately has shown to be one of the most effective ways to reduce the number of casualties. In addition, there have been significant limitations on the number of scans performed and the amount of time radiologists may spend analyzing the results to determine the severity of the diseases and potential future advancement due to the unexpected spike in cases. Thus methods are being investigated for automated techniques that could reduce some of the strain on the healthcare system to provide rapid and correct diagnoses. Moreover, identifying potential hotspots for such diseases in future can help in deciding upon micro-containment zones which can be a proactive step in hindering the rapid spread of the disease. Several machine learning and deep learning based approaches have been investigated for either classification or images or identifying potential hotspots. This paper presents a data driven method to classify Covid-19 images along with identifying potential pandemic hotspots so as to aid both the treatment process along with stopping spread of pandemics in the future. A comparative analysis has been presented with respect to present state of the art machine learning and deep learning algorithms to weigh the performance of the proposed approach. Results indicate the improved performance of the proposed data driven approach with probabilistic classification compared to baseline approaches.

Keywords: *Novel Coronavirus, COVID-19 Pandemic, Automated Detection, Probabilistic Classification, Deep Neural Networks.*

1. Introduction

Modern The human interaction with pandemics has been sporadic with the last pandemic encountered in recent history was the Spanish flu in the previous century [1]. The Covid-19 pandemic was a catastrophic occurrence of unprecedented measure wherein enormous losses of human life took place [2]. The situation catapulted to a massive financial recession and economic slowdown whose effects are being felt presently [3]. As the pandemic subsided with widespread containment zones, development of vaccines and development of herd immunity, it was realized that a much more proactive approach needs to be developed in order to deal with similar future events. There are important lessons to be gained from this current catastrophe in order to better anticipate and prepare for pandemics in the future [4]. The significance of early discovery and quick action is covered in the first important lesson. Before appropriate countermeasures could be put in place, COVID-19 was able to spread throughout the world due to the delayed awareness of its seriousness [5]. In order to quickly identify and address new threats, future pandemic preparedness should priorities strengthening surveillance systems, international collaboration, and information sharing [6].

[1,2]Department of Computer Science and Engineering
[1] Research Scholar, SAGE University, Indore
[2] Research Supervisor, SAGE University, Indore, (M.P.), India.
E-mail Id: [1] mathariya@gmail.com
E-mail Id: [2] drhemang.shrivastava@sageuniversity.in
[2] Corresponding Author: Mr. Sandeep Kumar Mathariya*
Email: mathariya@gmail.com

Numerous vulnerabilities were made apparent by the COVID-19 pandemic's burden on healthcare services. Investments in healthcare infrastructure, such as enough medical supplies, skilled medical personnel, and flexible systems that can handle spikes in cases, are necessary to prepare for future pandemics [7]. International cooperation and synchronization are critical. Because of the interdependence of today's world, fighting pandemics requires cooperation from all parties. It will be essential to manage and avert future health crises to enhance international cooperation in areas like vaccination distribution, data exchange, and resource allocation [8].

Technological developments in the fields of vaccine research, antiviral therapy, and diagnostic technologies are essential to being prepared for pandemics [9]. Maintaining a commitment to research and innovation will put the globe in a better position to respond to future pandemics [10]. A critically important finding of the present COVID-19 pandemic was the use of data driven machine learning models for both diagnosis and well as planning containment zones to stop the widespread and rapid spread of the disease. This paper presents a data driven approach which serves two major purposes [11]-[12]:

1. Classifying images as Covid positive or negative.
2. Analyzing data patters to evaluate the potential of a region to harbor high density Covid cases (becoming a hotspot).

These two objectives are imperative to fight pandemics in future, if need be. Machine Learning and Deep Leaning

based approaches have been explored to address the aforesaid problems and the results have been promising [13].

2. Related Work

Several approaches have been explored to classify CT or MRI image into Covid positive or negative cases employing statistical feature extraction followed by machine learning approaches or deep learning approaches. Moreover, data driven approaches have also been explored for predictive identification of potential hotspots. A brief summary of such approaches has been presented in table 1.

Table. 1 Summary of noteworthy contribution in the field.

Authors	Publication	Approach	Results and Finding
Zhang et al.	Elsevier 2022	A deep learning based approach to identify point of interest (POI) in epidemic hotspots.	Risk factors (features) used to train a generative adversarial network (GAN) to identify point of interest (POI) in urban areas.
Xu et al.	Elsevier 2022	A deep learning based model for forecasting future Covid cases.	Long Short Tem Memory (LSTM) obtained forecasting accuracies between 90% to 98% for different geographic locations.
Rashid et al.	Springer 2023	Analysis of novel Coronavirus using machine learning approaches.	Mean accuracy of 92.9% was obtained through supervised machine learning algorithms such a neural networks.
Mollaloa et al.	Elsevier 2021	Feature selection along with Support Vector Machine (SVM) employed for identifying the hotspots and age-adjusted mortality rates	Classification accuracy of 91% achieved through the SVM based approach which depicted quick performance saturation.
Khan et al.	MDPI 2020	A proactive approach in identifying potential hotspots prediction employing deep neural networks	Accuracy of 79% obtained through Long Short Term Memory (LSTM) model.
Akbarimajdet al.	Elsevier 2022	Convolutional Neural Network (CNN) with noise map layer to identify noisy and non-noisy pixel regions, for accurate classification	Accuracy of 72% achieved with impulse noise added X-Ray images which are difficult to analyse through conventional deep learning models such as CNN, SqeezeNet, and ResNet. Proposed approach beats ResNet 18 and ResNet 50 by 2%
Aslan et al.	Elsevier 2022	CNN and Bayesian Optimization	ghest accuracy of 96.29% achieved for Bayesian Optimization for Hyperparameters.
Momeny et al.	Elsevier 2021	Autoencoder based CNN to generate images with impulse and Gaussian noise for clearer demarcation of noise affected X-Ray images.	pposed system attains sensitivity of 0.808, specificity of 0.915, and F-Measure of 0.737.

Das et al.	Elsevier 2020	Transfer learning with Inception Net.	curacy of 97.406 attained for the Inception Net transfer learning model.
Zebari et al.	IEEE 2020	Feature extraction through Local Binary Pattern (LBP), Fractal Dimension (FD), and Grey Level Co-occurrence Matrices (GLCM) followed by classification by support vector machine (SVM)	P, FD and GLCM feature based classification attains accuracy of 89.87%, 87.84%, and 90.98% while the proposed fusion based features attain an accuracy of 96.91%.
Gannour et al.	IEEE 2020	Deep Learning Models VGGNet, InceptionNet, ExceptionNet, ResNet and MobileNet employed.	ghest accuracy of 97% attained with InceptionNet with ADAM optimizer.

3. Methodology

The proposed approach entails image-processing followed by feature extraction and classification to classify positive and negative cases [24]. While several deep learning approaches such as variants of CNNs are available at our disposal, yet the copious amounts of data and processing power needed to train the algorithms is extremely large to attain significantly high classification accuracy [25]. Alternatively an image processing based approach coupled with feature extraction is presented in this paper so as to overcome the challenge of extremely large datasets [26].

Data Pre-Processing

The first step though is the removal of noise from raw captured images, whose sources can be:

1) Addition of electronic noise in the image due to the use of amplifiers in the sensing device which is also termed as white or Gaussian noise [27].
2) The abrupt change or spikes in the analog to digital converters sued in the circuity of the fundus image causing salt and pepper noise patterns [28].
3) The multiplicative noise effect due to the inconsistent gain of the adaptive gain control (AGC) circuity used for capturing or retrieving the fundus image 29 [].
4) The lack of pixels while capturing the image resulting in frequency mean valued interpolations in the reconstructed image causing Poisson image [30]- [31].

The removal of noise effects is fundamentally important as noisy images would result in erroneous feature extraction leading to inaccurate classification of the CT/MRI images [32]. Contrary to conventional Fourier based methods, the wavelet transform is made us of non-smooth Kernel functions such as Mayer, Haar, Coif etc [33]-[34]. The essence of the transform lies in the fact that the wavelet transform separates the low frequency and high frequency components as the approximate co-efficient (C_A) and detailed co-efficient (C_D) of the transform. Generally, detailed co-efficient (C_D) and a low frequency resolution component termed as the detailed co-efficient (C_A) [35]..

Retaining the low frequency component(C_A) while discarding the higher frequency component(C_D) for a number of iterations helps in removal of the baseline noise of the system [36]. One of the most effective hyperspectral image restoration techniques is based on the sub-band decomposition of images into low pass and high pass signal values using the wavelet transform [37]. The wavelet transform, unlike the conventional Fourier methods uses non-linear and abruptly changing kernel functions which show efficacy in analysing abruptly fluctuating signals such as images. The continuous and the discrete wavelet transforms are computed as:

$$\boldsymbol{CWT(x,s,\delta) = s^{\frac{1}{2}} \int_{-\infty}^{\infty} x(t)\, \emptyset^*(\frac{t-s}{\delta})dt} \quad \textbf{(1)}$$

Where,

$s, \delta \in R$ represent the scaling (dilation) and shifting (translation) constants constrained to the condition $\delta \neq 0$.

$\emptyset^*$ is the Wavelet Family or Mother Wavelet

t is the time variable

$x(t)$ is the time domain data.

For implementing the wavelet transform on the image dataset, the sampled version of the continuous wavelet transform yields the discrete wavelet transform given by:

$$\boldsymbol{DWT(x,m,n) = \delta_0^{m\frac{-1}{2}} \sum_i x(i)\emptyset^* \left[\frac{n - is_0^m}{s_0^m}\right]} \quad \textbf{(2)}$$

Where,

$x(i)$ is the discrete $k \times 1$ vector.

s_0^m is the discrete scaling constant.

is_0^m is the discrete shifting constant.

The discrete wavelet transform yields two distinct low and high pass values based on the number of levels of decomposition and wavelet family given by the approximate co-efficient (CA) and detailed co-efficient (CD) [38]. The approximate co-efficient values are typically the low pass values containing the maximum information content of the image while the detailed co-efficient values account for the noisy spectral part. Retaining the low pass co-efficients and recursively discarding the high pass co-efficients allows to de-noise the image [39]. The choice of the wavelet family impacts the estimation of the noise gradient vector given by [40]:

$$\boldsymbol{G_N = k\frac{\nabla I}{\nabla I_F}} \quad \textbf{(3)}$$

The value of the second order normalizing gradient as a function of spatial co-ordinates is given by:

$$\boldsymbol{q(x,y) = \sqrt{\frac{c_1(\nabla I/I_F)^2 + c_2(\nabla^2 I/I_F)^2}{(1 + c_3(\nabla^2 I/I_F)^2}}} \quad \textbf{(4)}$$

Here,

I denotes the original image.

I_F denotes the fused image after normalization.

$\boldsymbol{G_N}$denotes the normalizing gradient.

∇ represents the gradient.

∇^2 represents the Laplacian.

Feature Extraction

The next step is the statistical feature extraction of image features expressed as [41]:

a) Mean or average value:

$$\boldsymbol{Mean\ or\ \mu = \frac{1}{N}\sum_i^N f_i X_i} \quad \textbf{(5)}$$

b) Standard Deviation:

$$\boldsymbol{sd = \sqrt{\frac{1}{N}\sum_i^N (X_i - \mu)^2}} \quad \textbf{(6)}$$

c) Energy which is also considered as the secondary moment:

$$\boldsymbol{Energy = \sum_{i,j}^n |A_{i,j}|^2} \quad \textbf{(7)}$$

d) Variance is the squared value of s.d. given by:

$$\boldsymbol{variance = sd^2} \quad \textbf{(8)}$$

e) Contrast which is the deviation among the mean and differential change in illuminance:

$$\boldsymbol{Contrast = \sqrt{\frac{1}{mn}\sum_{i,j}^{m,n}[X(i,j) - \mu(i,j)]^2}} \quad \textbf{(9)}$$

f) Entropy which is the statistical average information content defined as:

$$\boldsymbol{E = -P(I_{x,y}) log_2 I_{x,y}} \quad \textbf{(10)}$$

g) Homogeneity which is the similarity among the pixel value distribution:

$$\boldsymbol{H = \sum_{i,j}^{m,n} \frac{P_{I,J}}{1 - [i-j]^2}} \quad \textbf{(11)}$$

h) Correlation which is the similarity overlap among pixel values:

$$\boldsymbol{Correlation_{i,j} = \sum_{i,j}^{m,n} \frac{(i - u_x)(j - \mu_j)P_{j_{x,y}}}{sd_x sd_y}} \quad \textbf{(12)}$$

i) Root Mean Square Value which is defined as the squared root of the squared mean of values in the random distribution defined as:

$$\boldsymbol{rms = \sqrt{\frac{\sum_{i=1}^n X_i}{n}}} \quad \textbf{(13)}$$

The normalizing factor for the gray covariance matrix (GLCM) is defined as:

$$\boldsymbol{N = \frac{X_{i,j}}{\sum_{i=0}^{m-1}\sum_{j=0}^{n-1} * X_{i,j}}} \quad \textbf{(14)}$$

Here,

X_i denotes random variable X

f denotes the frequency of occurrence

$I_{x,y}$ denotes the image

m, n denotes pixels

$mean$ denotes avg. illuminance

A denotes the amplitude

N denotes levels of normalized GLCM matrix

$p_{i,j}$ denotes the normalized GLCM matrix

P denotes probability

The design of the automated classifier is critically important as the accuracy of classification critically depends on the design of the classifier. Generally, positive and negative

CT/MRI images show overlapping feature values. Hence a probabilistic approach is often effective. An image processing is practically carried out in hospitals to medical facilities, hence deep learning algorithms which need large computational resources may render infeasibility to even a novel and accurate approach [42]. This leads to a natural inclination towards the Bayesian Regularization algorithm [43].

the labelled data vector $Tr = [f_1 \dots \dots \dots . f_{12}]_{no\ of\ images}$ is fed to the bayesian regularized ann. the brann is chosen as it is an effective classifier. it works on the principle of Baye's theorem of conditional probability. After the BRANN is trained, in the testing phase, the BRANN calculates the probability of an element to belong to a particular category [44]. For a multi-class decision, the higher probability of a particular class decides the category of the data. In case of the BRANN tries to find out the probability of an image to be actually positive based on the probability before passing the judgement. For this, the important assumption which the BRANN makes is that of the accuracy of the classifier [45]. This is dependent on the training accuracy which is available to the classier (on completion of training) and the number of positive images in the dataset (already available to the classifier as the dataset provided by the user, which the classifier assumes to be true). The same logic applies to the negative images [46].

The training rule for the approach is based on the Bayes theorem of conditional probability which is effective for classifying overlapping feature vectors, based on a penalty $\boldsymbol{\rho} = \frac{\boldsymbol{\mu}}{\boldsymbol{v}}$. The weights are updated based on the modified regularized cost function [47]:

$$\boldsymbol{F(w) = \mu w^T w + v[\frac{1}{n}\sum_{i=1}^{n}(p_i - a_i)^2]} \quad \textbf{(15)}$$

If $(\pi \ll v)$: Network error are generally low.

else if $(\pi \geq v)$: Network errors tend to increase, in which case the weight magnitude should be reduced so as to limit errors (Penalty).

This is done be maximizing the weight Posteriori Probability using the Bayes theorem of Conditional Probability as:

$$\boldsymbol{P(\langle w|X \rangle,\ \mu,\ v)} \quad \textbf{(16)}$$

The proposed training algorithm is presented next.

Proposed Algorithm:

Step.1: Initialize weights $\boldsymbol{w}$ and learning rate $\boldsymbol{\mu}$ randomly, set maximum iterations as $\boldsymbol{Maxitr = 1000,\ e_{tolerance} = 10^{-6}}$

Step.2: $\boldsymbol{for}\ i = 1{:}\,Maxitr$, do

Step.3: $\boldsymbol{for\ (k = 1{:}\,n),}$

Step.4: Retain (C_A) while discarding (C_D)

Step.5: $Minimize\ (J = \overline{[\![x - WW^T x]\!]})$ and compute $M = B_{lxl}D$

Step.6: Compute $X_{LV} = mean(g(\sum X_{t-kh}), \epsilon_t)$

Step.7: $\boldsymbol{if}\ i \leq Maxitr$ && $if\ J \leq \boldsymbol{e_{tolerance}}$

Step.8: Minimize: $Argmin\left(\frac{\varepsilon_{inst} - \varepsilon_{opt}}{\varepsilon_{opt}}\right) \forall \alpha, \mu$

Step.9: Compute $w_{K+1} = w_k - \mu\beta(k)$

Step.10: Compute $\beta(k) = \alpha\beta(k-1) + \nabla C(w_k)$

Step.11: $else$

Step.12: Truncate training

Step.13: $\boldsymbol{end\ if}$

Step.14: Compute MSE, MAPE, R^2

Step.15: $\boldsymbol{end\ for}$

Step.16: $\boldsymbol{end\ for}$

The performance metrics to be computed are [47]:

Accuracy (Ac): It is mathematically defined as:

$$\boldsymbol{Ac = \frac{TP+TN}{TP+TN+FP+FN}} \quad \textbf{(17)}$$

Recall: It is mathematically defined as:

$$\boldsymbol{Recall = \frac{TP}{TP+FN}} \quad \textbf{(18)}$$

Precision: It is mathematically defined as:

$$\boldsymbol{Precisiosn = \frac{TP}{TP+FP}} \quad \textbf{(19)}$$

F-Measure: It is mathematically defined as:

$$\boldsymbol{F - Measure = \frac{2.Precision.Recall}{Precision+Recall}} \quad \textbf{(20)}$$

Here,

TP, TN, FP and FN denote the true positive, true negative, false positive and false negative rates respectively.

4 Experimental Results

The experiments are carried out of MATLAB 2022a with the Deep Learning Toolbox. The experiment is performed on a Windows Machine with i5-9300H Processor enabled with NVIDIA GTX GPU and RAM of 8GB. The software package used in Matrix Laboratory (Matlab), 2022a. For the purpose of this study, 1000 images comprising of both positive and negative cases of Covid have been used. The images are .jpg images in this experimental setup, but the system is compatible with all other common image data types such as .png, .tiff etc. The images acquired are .jpg

images which three colour channels viz. R, G and B. All the images are first converted to common dimensions of (256 x 256). The features are then used to train a Deep Bayes Net. The performance metrics chosen are the accuracy of classification and prediction error in terms of the TP, TN, FP and FN values respectively. The images are presented in the sequence of occurrence in the experimental setup followed by a detailed explanation and significance of each image obtained at each step.

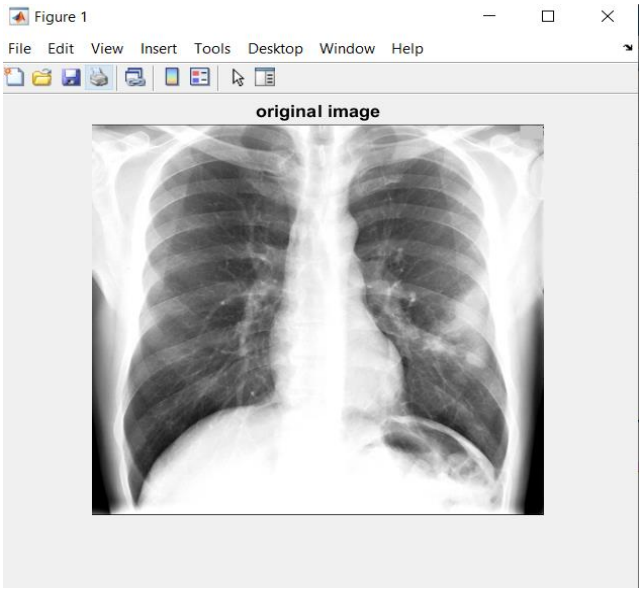

Fig.1 Original Image

Fig.2 Segmentation

Figure 1 depicts the original image while figure 2 depicts the segmented image, where the affected region in localized.

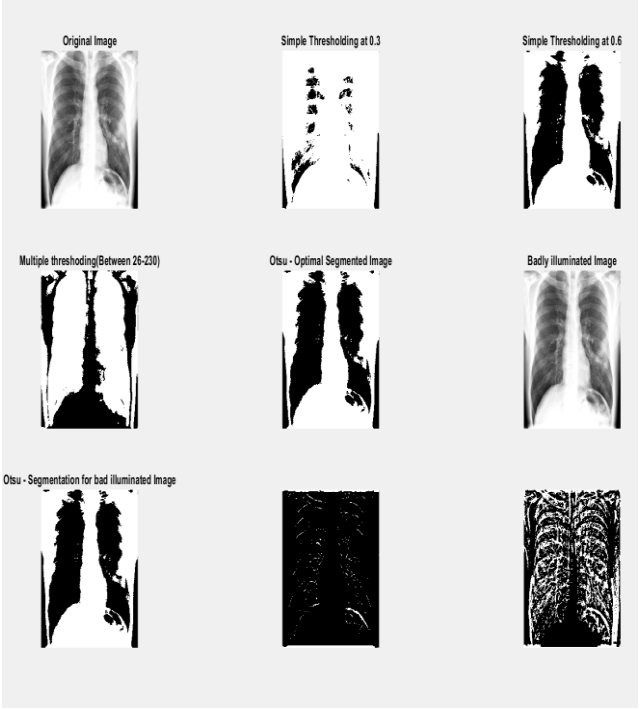

Fig.3 Variations in Segmentation based of threshold

Figure 3 depicts the various segmentation results on the image under interest.

The statistical features of the wavelet decomposition tabulated in table 2 followed by the image features computed subsequent to the DWT decomposition, in table 3.

Table.2 Statistical Analysis

S.No.	Parameter	Values	Class
1.	Minimum	0	Original Image
2.	Maximum	0.9295	
3.	Mean	0.3415	
4.	Median	0.3703	
5.	Standard Deviation	0.1524	
6	Mean Absolute Deviation	0.05355	
7.	Minimum	0.002951	Approximate Co-efficient values
8.	Maximum	0.9165	
9.	Mean	0.3415	
10.	Median	0.3706	
11.	Standard Deviation	0.1511	

12.	Mean Absolute Deviation	0.05354	
13.	Minimum	-0.1592	Detailed Co-efficient values
14.	Maximum	0.1592	
15.	Mean	0	
16.	Median	0	
17.	Standard Deviation	0.01232	
18.	Mean Absolute Deviation	0.005539	

After the DWT decomposition, the feature values of the images are to be computed as defined in the feature extraction section. The feature values computed from the images need to be fed to the proposed machine learning model for pattern recognition for both positive and negative cases. As an illustration, two separate CT images have been analysed using the proposed algorithm and their features have been tabulated in table 3. It can be observed that the statistical feature values have identical values for both positive and negative cases of covid, which necessitates the use of an accurate classifier.

Table.3 Image Features

Features	Normal Fundus Image	Glaucoma Fundus Image
Contrast	0.362500000000000	0.328409090909091
Correlation	0.151836572326215	0.179081293145884
Energy	0.700218879132232	0.723267045454546
Homogeneity	0.915729166666667	0.921979166666667
Mean	0.006526458817444 87	0.002272122187886 13
Standard Deviation	0.106429183594269	0.106604988215597
Entropy	3.53356796596205	3.43675888527571
RMS	0.106600358177805	0.106600358177805
Variance	0.011192908986343 5	0.011189247480491 1
Smoothness	0.923435573787053	0.807650945366392
Kurtosis	6.63089615157184	6.70718347384146
Skewness	0.512491012022217	0.483428823467213

Now, one of the most effective ways to ensure the accuracy and coherence of the feature extraction process is the distribution analysis of feature values for a multitude of images. Although there can be variations in images of a particular class of image in any dataset, yet the feature values should depict a certain amount of coherence over a multitude of images. Thus the feature sets for multiple images in the dataset (taken 10 for the sake of brevity and ease of analysis) has been depicted in figure 12. Figure 12 clearly indicates a similarity in the values of the features extracted from the images. For instance, feature 1 (for all the 10 images) clearly show a much lesser magnitude of value compared to feature 11 as depicted in figure 12.

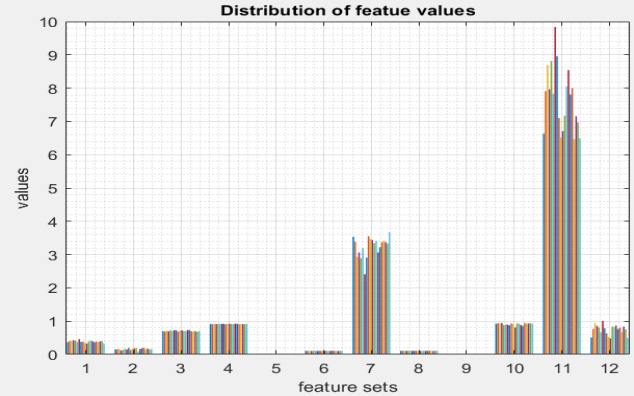

Fig.4 Distribution of feature values

A similar analysis can be done using the mesh plot depicted in figure 8. The mesh renders a three dimensional view of the feature value distribution. A coherent inference can be drawn from figures 7 and 8 depicting the fact that the feature distribution for similar class of features over a multitude of images show similarity in values. For instance, feature 1 (for multiple images) shows much lesser value compared to feature 11 (for multiple images). This is the exact same illustration taken in figure 4.

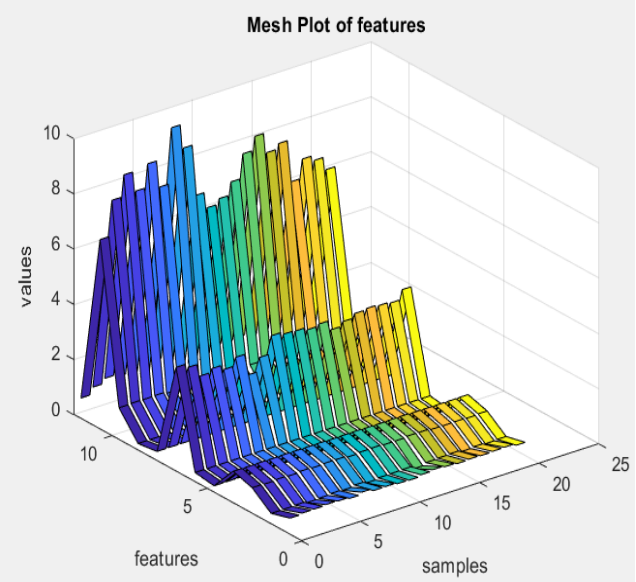

Fig.5 Mesh Plot of features

As machine learning algorithms often suffer from imbalanced instances, this phenomenon has been carefully considered while data set preparation. Imbalanced instances to imbalanced class distributions occur when the samples or observations of one of the classes is either much higher or much lower compared to the other class or classes. This may result in misleading results as machine learning algorithms tend to statistically ignore the class distributions. This caveat is eliminated in this experiment by following almost an equal share of glaucoma positive and negative image classes. This can also been seen in the confusion matrix for the testing case. As the positive and negative cases have an identical class distribution, hence resampling (over sampling, under sampling or SMOTE (Synthetic Minority Oversampling Technique) has not been performed.

Three sub cases of the discriminant analysis are again considered in this experiment which happen to be:

1) Linear Discriminants.

2) Quadratic Discriminants.

3) Optimizable Discriminants.

It is observed that for a parallel pools for the training, the 3 case feature selection attains convergence in 30 iterations. The linear discriminant results in an accuracy of 98%, the quadratic discriminant results in an accuracy of 97.33% and the optimizable discriminant results in an accuracy of 98%.

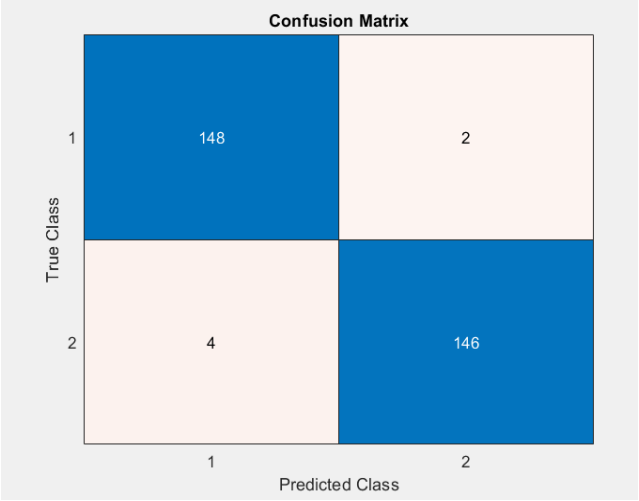

Fig, 6 Confusion Matrix for Image Classification

The performance of the proposed approach is can be evaluated in terms of the true positive (TP), true negative (TN), false positive (FP) and false negative (FN) rates of the confusion matrix. Out of the 1000 images of the dataset, 70% i.e. 700 images have been used for training and the rest of the 30% i.e. 300 images have been used for testing. The TP, TN, FP and FN values are depicted in the Confusion Matrix in figure 9. Based on the TP, TN, FP and FN values, the accuracy, sensitivity/recall, specificity, precision and F-Measure values have been computed and tabulated in table 5. The proposed approach attains an accuracy of 0.98, sensitivity or recall value of 0.9866, specificity of 0.9733, precision of 0.9736 and F-Measure of 0.9800. The mean training time for the proposed approach has been 12 minutes for the training dataset alone.

Table 4 Performance Metrics

Accuracy%	**Sensitivity Or Recall %**	**Specificity%**	**Precision%**	**F-Measure**
0.980	0.9866	.9733	.9736	.9800

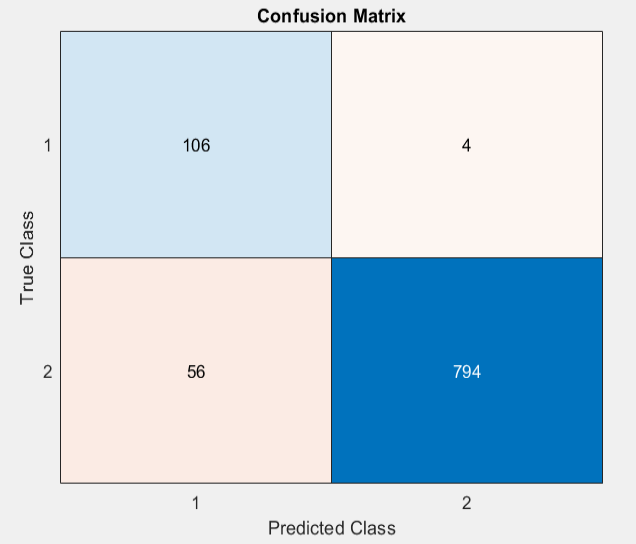

Fig.8. Confusion matrix for hotspot identification

While there can be many more parameters which may affect the area to be a hotspot, the above parameters are the most significant. The data parameters employed in this study are:

1. Age Bracket
2. Gender
3. Detected Area
4. Detected State
5. Current Status
6. Travel History
7. Contacted From
8. Nationality
9. Type of Transmission
10. Identity
11. No. of Cases
12. Containment Zone (target)

The approach attains a classification accuracy of 93.75% for the hotspot identification. To evaluate the performance of the proposed work in comparison to the contemporary approaches in the domain has been presented in table 5.

Table 5 Comparative Analysis w.r.t. existing work

Method	**Accuracy**
Mollaloa et al. (2021)	91%
Kahn et al. (2020)	79%
Alsan et al. (2022)	96.29
Akbarimajd et al. (2022)	72%
Momeny et al. (2021)	80.8%
Das et al. (2020)	97.4%
Zebari et al. (2022)	89.87%
Gannour et al.	97%
Proposed	**98%**

Table 5 presents a comparative study with respect to contemporary existing work in the domain. It can be observed from table 5 that the proposed work attains relative higher accuracy compared to existing methods in the domain. The improvement in the results can be attributed to the following reasons:

1) Image enhancement employing illumination correction and histogram normalization compensating inconsistencies in fundus image capturing.

2) Iterative noise removal for denoising fundus images for accurate feature extraction.

3) Computing stochastic feature and subsequent feature optimization to enhance the training efficacy.

4) While deep learning models such as the CNN, RCNN, ResNet etc. may have the advantage of avoiding additional effort in handpicking features and feature combinations, they lose control over choosing the features to be used to train a model. The proposed approach with stochastic features to train a Bayesian Deep Neural Network attains relatively higher accuracy of classification compared to benchmark techniques. Moreover, the approach is also capable of identifying potential hotspots based on geographical and statistical survey features with an accuracy of 93.75%

5. Conclusion

It can be concluded from previous discussions that the onset of the pandemic has seen several changes globally with severe effects on the healthcare and financial sectors. Complete lockdowns have been prevalent globally to restrict the spread of the virus among large populations This would allow in implementing smart lockdowns rather than complete lockdowns thereby causing a less severe impact on financial and economic conditions. The task is challenging owing to the fact that the multitude of parameters in the hotspot data sets are highly uncorrelated. However, an optimized model would allow identifying possible hotspots in future pandemic or epidemic like situations. Thus, identifying Hotspots accurately is necessary for smart lockdowns, restricting more outbreaks, better containment and effective travel guidelines. Additionally, development of machine learning and deep learning based approaches which can accurately classify

CT/MRI images would greatly assist medical practitioners in early detection and isolation of patients.

The purpose of the work is to design a low computational complexity based method for automated glaucoma detection which can be implemented practically on hardware constrained platforms as well. Rigorous image denoising, feature computation and optimization has been implemented to train a deep neural network. The Deep Bayes Net has been used as it serves as an effective classifier for overlapping boundary datasets. It has been shown that the proposed system attains a classification accuracy of 98% which is at par with existing work in the domain. The approach also attains a classification accuracy of 93.75% in identifying potential future hotspots. Future enhancements of the work can be employing self-supervised (SSL) learning methods which would in turn reduce the time and effort in manual labelling of the datasets.

Author contributions

Mr. Sandeep Kumar Maharaja: Data collection, Implementation of proposed model, compilation of results and drafting manuscript.

Dr. Hemang Shrivastava: Conceptualization of Research Problem and Methodology, Writing-Reviewing and Editing.

Conflicts of interest

The authors declare no conflicts of interest.

References

[1] J. Miah, R. H. Khan, S. Ahmed and M. I. Mahmud, "A comparative study of Detecting Covid 19 by Using Chest X-ray Images– A Deep Learning Approach," 2023 IEEE World AI IoT Congress (AIIoT), Seattle, WA, USA, 2023, pp. 0311-0316

[2] A. Hussain, S. U. Amin, H. Lee, A. Khan, N. F. Khan and S. Seo, "An Automated Chest X-Ray Image Analysis for Covid-19 and Pneumonia Diagnosis Using Deep Ensemble Strategy," in IEEE Access, 2023, vol. 11, pp. 97207-97220,.

[3] S. Mishra and A. Mantri, "Design of COVID19 Detection based on Relative Eccentric Feature Selection using Deep Vectorized Regressive Neural Network for Corona Virus," 2023 IEEE International Conference on Integrated Circuits and Communication Systems (ICICACS), Raichur, India, 2023, pp. 1-6.

[4] J Somasekar, PP Kumar, A Sharma, "Machine learning and image analysis applications in the fight against COVID-19 pandemic: Datasets, research directions, challenges and opportunities", Proceedings in Matrials Today, Elsevier 2021.

[5] J. De Moura et al., "Deep Convolutional Approaches for the Analysis of COVID-19 Using Chest X-Ray Images From Portable Devices," in IEEE Access, 2020, vol. 8, pp. 195594-195607

[6] S Kumar, RD Raut, BE Narkhede," A proposed collaborative framework by using artificial intelligence-internet of things (AI-IoT) in COVID-19 pandemic situation for healthcare workers", International Journal of Healthcare Management, Taylor and Francis, 2020, vol.13, no.4, pp. 337-345.

[7] JB Awotunde, SO Folorunso, RG Jimoh, "Application of artificial intelligence for COVID-19 epidemic: an exploratory study, opportunities, challenges, and future prospects", Artificial Intelligence for COVID-19. Studies in Systems, Decision and Control, Springer, 2021, vol 358.

[8] S. Hu et al., "Weakly Supervised Deep Learning for COVID-19 Infection Detection and Classification From CT Images," in IEEE Access, 2020, vol. 8, pp. 118869-118883.

[9] J. C. Clement, V. Ponnusamy, K. C. Sriharipriya and R. Nandakumar, "A Survey on Mathematical, Machine Learning and Deep Learning Models for COVID-19 Transmission and Diagnosis," in IEEE Reviews in Biomedical Engineering, 2022, vol. 15, pp. 325-340.

[10] H. S. Alghamdi, G. Amoudi, S. Elhag, K. Saeedi and J. Nasser, "Deep Learning Approaches for Detecting COVID-19 From Chest X-Ray Images: A Survey," in IEEE Access, 2021, vol. 9, pp. 20235-20254.

[11] T Ozturk, M Talo, EA Yildirim, UB Baloglu, "Automated detection of COVID-19 cases using deep neural networks with X-ray images", Computers and Biology and Medicine, Elsevier 2020, col.121, 103792.

[12] J. C. Clement, V. Ponnusamy, K. C. Sriharipriya and R. Nandakumar, "A Survey on Mathematical, Machine Learning and Deep Learning Models for COVID-19 Transmission and Diagnosis," in IEEE Reviews in Biomedical Engineering, 2022, vol. 15, pp. 325-340

[13] M. M. Islam, F. Karray, R. Alhajj and J. Zeng, "A Review on Deep Learning Techniques for the Diagnosis of Novel Coronavirus (COVID-19)," in IEEE Access, vol. 9, pp. 30551-30572.

[14] Y Zhang, Q Zhang, Y Zhao, Y Deng, H Zheng, "Urban spatial risk prediction and optimization analysis of POI based on deep learning from the perspective of an epidemic", International Journal of Applied Earth Observation and Geoinformation, , Elsevier, 2022, vol. 112, 102942.

[15] L Xu, R Magar, AB Farimani, “Forecasting COVID-19 new cases using deep learning methods”, Computers in biology and medicine, Elsevier 2022, vol.144, 105342

[16] AS Kwekha-Rashid, HN Abduljabbar, B Alhayani, “Coronavirus disease (COVID-19) cases analysis using machine-learning applications”, Applied Nanoscience, Springer, 2023, vol.31, pp. 2013–2025.

[17] A Mollalo, B Vahedi, S Bhattarai, LC Hopkins, “Predicting the hotspots of age-adjusted mortality rates of lower respiratory infection across the continental United States: Integration of GIS, spatial statistics and machine learning algorithms”, International Journal of Medical Informatics, Elsevier, 2021, vol. 142, 104248.

[18] SD Khan, L Alarabi, S Basalamah -, “Toward Smart Lockdown: A Novel Approach for COVID-19 Hotspots Prediction Using a Deep Hybrid Neural Network”, Journal of Computers, MDPI, 2020, vol.9, no.9, pp1-16.

[19] A Akbarimajd, N Hoertel, MA Hussain, “Learning-to-augment incorporated noise-robust deep CNN for detection of COVID-19 in noisy X-ray images”, Journal of Computational Science, Elsevier 2022, vol.63, 101763.

[20] M Momeny, AA Neshat, MA Hussain, S Kia, “Learning-to-augment strategy using noisy and denoised data: Improving generalizability of deep CNN for the detection of COVID-19 in X-ray images”, Computers in Biology and Medicine, Elsevier, 2022, vol.136, 104704.

[21] MF Aslan, MF Unlersen, K Sabanci, A Durdu, “CNN-based transfer learning–BiLSTM

[22] NN Das, N Kumar, M Kaur, V Kumar, D Singh, “Automated deep transfer learning-based approach for detection of COVID-19 infection in chest X-rays”, IBRM, Elsevier, 2022, vol.43, no.2, pp.114-119.

[23] D. A. Zebari, A. M. Abdulazeez, D. Q. Zeebaree and M. S. Salih, "A Fusion Scheme of Texture Features for COVID-19 Detection of CT Scan Images," 2020 International Conference on Advanced Science and Engineering (ICOASE), 2020, pp. 1-6.

[24] O. El Gannour, S. Hamida, B. Cherradi, A. Raihani And H. Moujahid, "Performance Evaluation of Transfer Learning Technique for Automatic Detection of Patients with COVID-19 on X-Ray Images," 2020 IEEE 2nd International Conference on Electronics, Control, Optimization and Computer Science (ICECOCS), 2020, pp. 1-6.

[25] SH Kassania, PH Kassanib, MJ Wesolowskic, “Automatic detection of coronavirus disease (COVID-19) in X-ray and CT images: a machine learning based approach”, Biometrics and Biomedical Engineering, Elsevier, 2021, vol.41, no.3, pp. 867-879.

[26] V Bolon-Canedo, B Remeseiro, “Feature selection in image analysis: a survey”, Artificial Intelligence Review, Springer 2020, vol. 53, pp. 2905–2931.

[27] R. Miikkulainen, J Liang, E Meyerson, A Rawal, “Evolving deep neural networks”, Artifical Intelligence in the Age of Neural Networks and Brain Computing, Academic Press, 2019, pp.293-312.

[28] A Zargari Khuzani, M Heidari, SA Shariati, “COVID-Classifier: An automated machine learning model to assist in the diagnosis of COVID-19 infection in chest x-ray images”, Scientific Repots, Nature, 2021, vol.11, no. 9887.

[29] M Shafiq-ul-Hassan, GG Zhang, K Latifi, “Intrinsic dependencies of CT radiomic features on voxel size and number of gray levels”, Scientific Reports, Nature, 2018, vol.8, no. 10545.

[30] M Toğaçar, B Ergen, Z Cömert, “COVID-19 detection using deep learning models to exploit Social Mimic Optimization and structured chest X-ray images using fuzzy color and stacking approaches”, Computers in Biology and Medicine, Elsevier 2020, vol.121, 103805.

[31] SH Kassania, PH Kassanib, MJ Wesolowskic, “Automatic detection of coronavirus disease (COVID-19) in X-ray and CT images: a machine learning based approach”, Biometrics and Biomedical Engineering, Elsevier 2021, vol.41, no.3, pp. 867-879.

[32] E. -S. M. El-Kenawy et al., "Advanced Meta-Heuristics, Convolutional Neural Networks, and Feature Selectors for Efficient COVID-19 X-Ray Chest Image Classification," in IEEE Access, 2021, vol. 9, pp. 36019-36037.

[33] K. K. Singh and A. Singh, "Diagnosis of COVID-19 from chest X-ray images using wavelets-based depthwise convolution network," in Big Data Mining and Analytics, 2021, vol. 4, no. 2, pp. 84-93.

[34] B. King, S. Barve, A. Ford and R. Jha, "Unsupervised Clustering of COVID-19 Chest X-Ray Images with a Self-Organizing Feature Map," 2020 IEEE 63rd International Midwest Symposium on Circuits and Systems (MWSCAS), 2020, pp. 395-398.

[35] ALA Dalal, MAA Al-qaness, Z Cai, EA Alawamy, “IDA: Improving distribution analysis for reducing data complexity and dimensionality in hyperspectral images”, Pattern Recogniton, Elsevier 2023, vol.134, no. 109096.

[36] R Mostafiz, MS Uddin, MM Reza, MM Rahman, “Covid-19 detection in chest X-ray through random forest classifier using a hybridization of deep CNN and DWT optimized features”, Journal of King Saud University - Computer and Information Sciences, Elsevier 2022, vol.34, no.6, Part B, pp. 3226-3235.

[37] U Muhammad, MZ Hoque, M Oussalah, “SAM: Self-augmentation mechanism for COVID-19 detection using chest X-ray images”, Lnowledge Based Systems, Elsevier 2022, vol.241, 108207.

[38] I. Ahmad, M. Basheri, M. J. Iqbal and A. Rahim, "Performance Comparison of Support Vector Machine, Random Forest, and Extreme Learning Machine for Intrusion Detection," in IEEE Access 2018, vol. 6, pp. 33789-33795.

[39] P. Padilla, M. Lopez, J. M. Gorriz, J. Ramirez, D. Salas-Gonzalez and I. Alvarez, "NMF-SVM Based CAD Tool Applied to Functional Brain Images for the Diagnosis of Alzheimer's Disease," in IEEE Transactions on Medical Imaging, 2012 vol. 31, no. 2, pp. 207-216

[40] G. Rathee, S. Garg, G. Kaddoum, Y. Wu, D. N. K. Jayakody and A. Alamri, "ANN Assisted-IoT Enabled COVID-19 Patient Monitoring," in IEEE Access, vol. 9, pp. 42483-42492.

[41] C. Zhou, J. Song, S. Zhou, Z. Zhang and J. Xing, "COVID-19 Detection Based on Image Regrouping and Resnet-SVM Using Chest X-Ray Images," in IEEE Access, 2021, vol. 9, pp. 81902-8191.

[42] S. K. Zhou et al., "A Review of Deep Learning in Medical Imaging: Imaging Traits, Technology Trends, Case Studies With Progress Highlights, and Future Promises," in Proceedings of the IEEE, 2021, vol. 109, no. 5, pp. 820-838.

[43] S. Tiwari, P. Chanak and S. K. Singh, "A Review of the Machine Learning Algorithms for Covid-19 Case Analysis," in IEEE Transactions on Artificial Intelligence.

[44] T. Sercu, C. Puhrsch, B. Kingsbury and Y. LeCun, "Very deep multilingual convolutional neural networks for LVCSR," 2016 IEEE International Conference on Acoustics, Speech and Signal Processing (ICASSP), 2016, pp. 4955-4959.

[45] MA Kızrak, Z Müftüoğlu, T Yıldırım, “Limitations and challenges on the diagnosis of COVID-19 using radiology images and deep learning”, Data Science for COVID-19, Computational Perspectives , Science Direct 2021, pp.91-115.

[46] K. Sanjar, A. Rehman, A. Paul and K. JeongHong, "Weight Dropout for Preventing Neural Networks from Overfitting," 2020 8th International Conference on Orange Technology (ICOT), Daegu, Korea (South), 2020, pp. 1-4.

[47] L Borawar, R Kaur, “ResNet: Solving Vanishing Gradient in Deep Networks”, Proceedings of International Conference on Recent Trends in Computing, Springer 2023, pp 235–247.